Slow dynamics and anomalous nonlinear fast dynamics in diverse solids

Paul Johnson[a)]
Geophysics Group, University of California, Los Alamos National Laboratory, Los Alamos, New Mexico 87545

Alexander Sutin[b)]
Davidson Laboratory, Stevens Institute of Technology, Hoboken, New Jersey 07030

(Received 19 April 2004; revised 27 September 2004; accepted 3 October 2004)

Results are reported of the first systematic study of anomalous nonlinear fast dynamics and slow dynamics in a number of solids. Observations are presented from seven diverse materials showing that anomalous nonlinear fast dynamics (ANFD) and slow dynamics (SD) occur together, significantly expanding the nonlinear mesoscopic elasticity class. The materials include samples of gray iron, alumina ceramic, quartzite, cracked Pyrex, marble, sintered metal, and perovskite ceramic. In addition, it is shown that materials which exhibit ANFD have very similar ratios of amplitude-dependent internal-friction to the resonance-frequency shift with strain amplitude. The ratios range between 0.28 and 0.63, except for cracked Pyrex glass, which exhibits a ratio of 1.1, and the ratio appears to be a material characteristic. The ratio of internal friction to resonance frequency shift as a function of time during SD is time independent, ranging from 0.23 to 0.43 for the materials studied. © *2005 Acoustical Society of America.* [DOI: 10.1121/1.1823351]

PACS numbers: 43.25.Dc, 43.25.Ba, 43.25.Ed, 43.25.Gf [MFH] Pages: 124–130

I. INTRODUCTION

The application of an oscillatory-wave or impulsive source at small strains to a solid that manifests nonlinear mesoscopic elastic behavior leads to a modulus and quality factor (inverse dissipation, Q) decrease.[1] Simultaneously, the elastic wave present in the material distorts, manifest by wave speed decrease, and the creation of harmonics and wave modulation.[1] Further, conditioning, an effect of strain memory is induced, manifest, for example, by resonant curve sweeps being different depending on whether the sweep is upgoing or downgoing in frequency.[2,3] These manifestations are *signatures of anomalous nonlinear fast dynamics* (ANFD), also termed *nonclassical nonlinear fast dynamics*.[4] The modulus and dissipation changes do not return to the initial values, the equilibrium state, after wave excitation terminates, but recover over 10^3-10^4 s with a log(time) dependence. This behavior is called *slow dynamics* (SD).[3]

In previous work,[1,5] it was speculated that SD always occurs in tandem with ANFD in nonlinear mesoscopic elastic materials. This has never been demonstrated aside from in a handful of materials. What has been demonstrated is that many materials exhibit ANFD, including sandstones and limestones,[2] damaged solids,[6,7] and concrete.[8] Slow dynamics have been described in sandstone and concrete[9] and in cracked sintered metal.[10] In fact, no systematic studies exist that characterize the connection between ANFD/SD. ANFD/SD has only been described in Berea sandstone,[3] and cracked Pyrex glass[11] to our knowledge.

The purpose of this paper is to report new measurements of ANFD/SD in diverse solids and establish a quantitative connection between ANFD and SD. In Sec. II, we describe SD/ANFD and provide relevant background information. In Secs. III and IV we present the experiment and results, and in Sec. V we discuss the results, and then conclude.

II. NONLINEAR DYNAMICS

A. Nonlinear fast dynamics in classical (atomic elastic) materials

The classical nonlinear theory for ''atomic elasticity'' (anharmonicity) used to describe nonlinear behavior in air, water, single crystals, etc., is thoroughly described in the literature,[12] and we will provide only a brief overview. The classical theory begins with the expansion of the elastic strain energy, E, in powers of the strain tensor, ϵ_{ij}. The expansion coefficients designate the components of the second-order elastic tensor and the third-order elastic tensor, respectively. These tensors are characterized, respectively, by 21 and 56 independent components for an arbitrary anisotropic medium (in the lowest-order, triclinic material symmetry) and by two and, respectively, three components in the highest-order symmetry (isotropic material).

The equation of motion in Lagrangian coordinates is

$$\rho\ddot{u}_i=\frac{\partial\sigma_{ij}}{\partial x_j}, \tag{1}$$

where ρ, σ_{ij}, and $\ddot{u}$ designate the density, the stress tensor, and the particle acceleration, respectively.

A one-dimensional, longitudinal wave (P-wave) propagating in an isotropic medium can exist with only nonzero components $\sigma_{xx}=\sigma$ and $u_x=u$ or $\epsilon_{xx}=\epsilon=\partial u/\partial x$. The corresponding equation of motion can be written as

$$\rho_0\frac{\partial^2\epsilon}{\partial t^2}=\frac{\partial^2\sigma(\epsilon)}{\partial x^2}. \tag{2}$$

a)Electronic address: paj@lanl.gov
b)Electronic address: asutin@stevens-tech.edu

From the energy expansion, the stress-strain relation (also known as the equation of state,) can be written as

$$\sigma = M(\epsilon + \beta\epsilon^2 + \delta\epsilon^3 + \cdots), \tag{3}$$

where M is the elastic modulus, and β and δ are nonlinear coefficients that can be expressed in terms of combinations of the higher order elastic moduli. This equation implies characteristic scaling relations. These are: (a) the amplitude of the second harmonic scales as ϵ^2; (b) the amplitude of the third harmonic scales as ϵ^3; and (c) the change in resonance frequency of the fundamental-mode resonance peak in a Young's mode experiment, for example, scales as ϵ^2.

B. Anomalous nonlinear fast dynamics

The behavior of nonlinear mesoscopic elastic (NME) materials is described in many articles.[1,5] These materials, the prototypical material being rock, behave in unexpected manners. At lower strain amplitudes (order 10^{-6} and lower) it has recently been shown that at least some nonlinear mesoscopic elastic materials (e.g., Berea sandstone) behave ''classically''[13] (obey Landau theory).[12] At higher strain amplitudes (order 10^{-6} and above) there is ample evidence suggesting that classical theory does not describe wave behaviors,[5,1,7] based on (i) observations of the scaling of harmonics and resonant peak shift with strain amplitude and (ii) the presence of conditioning. A mean field theory developed by McCall and Guyer[14] has been broadly applied to both quasistatic and dynamic behavior in these materials, over part of the dynamic strain range.[1,6,7,15] In this region, hysteresis in the equation of state has been appealed to and can be included in the following manner:

$$\sigma = M(\epsilon + \beta\epsilon^2 + \cdots) + \hat{\alpha}[\epsilon, \mathrm{sign}(\dot{\epsilon})], \tag{4}$$

where $\hat{\alpha}$ is a function describing hysteresis in $\sigma - \epsilon$, a ''nonclassical'' effect.[1] This function depends on whether stress is increasing or decreasing and thus the sign term, $\dot{\epsilon} = \partial\epsilon/\partial t$. A specific form of α should follow from the material physics, not yet established.

The above approach does not include conditioning. Conditioning is an induced, continuous state of disequilibrium during dynamic excitation of NME materials. Meaning, that when the sample is excited by an elastic wave, the modulus, and Q decrease immediately; however, if the excitation continues, the modulus and Q continue to decrease for some period of time until the material reaches a new equilibrium state where no more change takes place. Conditioning is considered by many to be the manifestation of slow dynamics during wave excitation, although this has not been quantitatively demonstrated. Existing theories that address conditioning include those described by Scalerandi and Delsanto[4] and Vakhnenko *et al.*[16] The recent model of Vaknenko *et al.* is based on the physics of bond rupture as the underlying mechanism of ANFD/SD. The ramifications of conditioning in ANFD are only beginning to be unraveled experimentally however, and will not be addressed further here, except to say our group is working on separating ANFD and SD at present. This issue does not affect the results described in this paper, but will ultimately affect the accompanying theory.

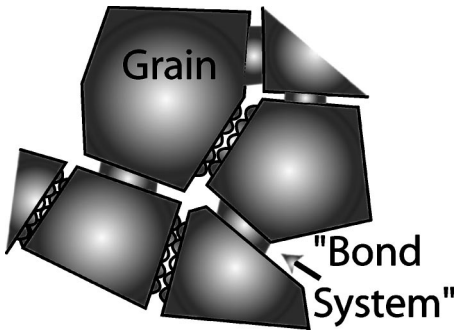

FIG. 1. The hard/soft paradigm of nonclassical materials.

C. Slow dynamics

We currently believe that, in the strain regime where ANFD takes place, SD also appears, manifest by a modulus recovery over $10^3 - 10^4$ s that is linear with $\log(t)$, commencing when a relatively strong wave excitation terminates. Whether the two behaviors appear simultaneously with strain level has not yet been experimentally verified, however, and this is a topic our group is currently working on. SD differs from the well-known phenomenon of creep observed in quasistatic experiments in rock and some metals[17] although they may well be related. SD is a mechanically induced behavior at very small dynamic strain levels, that displays asymmetry with respect to the driving excitation stress. That is, the modulus always displays a quasistatic decrease in response to fast, symmetric oscillatory driving stress. The observed asymmetry is contrary to other physical systems that display proportion to the $\log(t)$ such as creep in rock[18] and metals,[19] magnetic fields, in spin glasses,[20] etc., that respond symmetrically to the driving stress.

The materials that exhibit ANFD and SD have in common a small volume of elastically soft constituents (e.g., bonds in a sintered ceramic) where the SD and ANFD originate, distributed within a rigid matrix (e.g., grains in the ceramic) as is shown in Fig. 1. We refer to this as the ''hard/soft'' paradigm. The soft portion of the material, the ''bond system''[1] is distributed throughout, but within a small fraction of the total volume, less than 1%. In cracked materials the bond system is localized.

III. EXPERIMENT AND DATA ANALYSIS

Our first step was to test a large number of samples (50–100) of a variety of solids to determine whether or not they exhibited ANFD/SD. The samples included numerous rock types, metals, and ceramics. Seven materials seen to exhibit ANFD were selected for quantitative study because they represent the enormous contrasting physical, geometrical, and chemical diversity of the class. These include a pearlite/graphite mixed phase metal (commonly called ''gray iron''), a 99.9% pure alumina ceramic (crucible material), a perovskite ceramic ($LaCoO_3$, used in oxygen separation and solid oxide fuel cells) a feldspathic quartzite, a sintered metal (used in bearings), a sample of Carrera marble (metamorphosed limestone) composed principally of calcite, and Pyrex glass containing a localized crack. Sample shape, dimension and physical characteristics are given in Table I.

TABLE I. Sample information for the seven materials studied. OD and ID refer to the outside and inside diameters, respectively, and L is sample length.

Material	Sample shape	Dimensions (mm^3)
Pearlite/graphite metal	Parallelepiped	100×14×9
Alumina ceramic	Rod	279×19
Quartzite	Rod	117×31.7
Pyrex containing cracks	Rod	284×16
Marble	Rod	101×22
Sintered metal	Ring	OD 41, ID 29, L 25
Perovskite ceramic	Parallellapiped	47.3×6.6×6.6

The experimental configuration used for ANFD and SD measurements is shown in Fig. 2. This setup provides the means to conduct ANFD and SD tests successively for each sample under the same conditions using the same equipment. For ANFD measurements, nonlinear resonant ultrasound spectroscopy (NRUS) was employed.[1,5,6] Using NRUS, the sample was continuously probed using a swept-frequency wave at an eigenmode of the material, applying progressively increasing drive levels. For these measurements we used the resonant ultrasound spectroscopy device manufactured by Dynamic Resonance Systems, Inc. The time-average amplitude for of sweep frequency is recorded and stored on computer. Samples were excited using piezoceramics bonded with epoxy. We used a laser vibrometer manufactured by Polytech for noncontact signal detection. Particle velocity $\dot{u}$ was measured with the Polytech, and $\hat{\epsilon}$, the dynamic strain amplitude, was calculated from this and wavespeed c,[1] $\hat{\epsilon}=\dot{u}/c$.

The linear (low amplitude) resonance frequency f_0 and its corresponding strain $\hat{\epsilon}_0$ were obtained by fitting the resonance peak with a lorentzian. Q, the most commonly applied measure of wave dissipation,[21] was obtained as follows. The Q of a linear elastic system is, $Q_0=2\pi f_0 W/\Delta W$. ΔW is the energy loss per cycle, W is elastic energy stored at maximum stress and strain during harmonic excitation, and f_0 is the mode frequency.[21] This also means that Q_0 is proportional to the wave amplitude at resonance for a given applied force. In a dynamic resonant system, $Q_0=2\pi f_0 W/\delta W=f_0/\delta f$, where δf is the frequency width between half power (3 dB in amplitude) about the resonance peak at f_0 on a power-frequency plot. When the system is linear we can apply a Lorentzian fit to extract Q_0. In a nonlinear system, however, $Q_0=f_0/\delta f$, cannot be used. In fact, definitions of nonlinear dissipation are normally obtained from the ringdown of a freely resonating body.[22–24] Since we have a continuously driven system, we must apply a different approach. In the elastically nonlinear case one can measure the power required to maintain a constant amplitude of oscillation.[22,24]

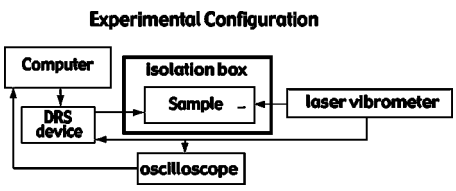

FIG. 2. Experimental configuration for ANFD/SD studies.

This is equivalent to measuring the amplitude of oscillation at constant applied force. In our system, the applied force F of the transducer attached to a solid sample is

$$F=\frac{m\ddot{u}}{2}, \tag{5}$$

where $\ddot{u}$ is acceleration of the transducer and m is its mass (we use no backload on the transducer). The applied force is constant over the frequency range of the experiment because we are operating well below the resonance frequency of the transducer. Further the force is proportional to the applied voltage V:

$$F=\frac{md_{33}\omega^2 V}{2}=k_1 V, \tag{6}$$

where d_{33} is the piezoelectric constant (in units of m/V) and ω^2 appears from calculating displacement u from acceleration $\ddot{u}$, and $k_1=md_{11}\omega^2/2$. The linear relation between force and voltage was verified experimentally.

At the far end of the bar, the detected strain amplitude $\hat{\epsilon}$ is related to the drive force by the amplitude dependent $Q(\hat{\epsilon})$ of the bar

$$\hat{\epsilon}=k_2 F Q(\hat{\epsilon}), \tag{7}$$

where k_2 is the transfer function of the bar.

Substituting Eq. (6) into Eq. (7) yields

$$\hat{\epsilon}=KVQ(\hat{\epsilon}), \tag{8}$$

where $K=k_1k_2$.

An advantage of this method is that k_1 and k_2 do not have to be measured. We can obtain K from the low amplitude measures of strain, voltage and Q_0 [obtained from the half width of the low amplitude (linear) resonance curve]

$$K=\frac{\hat{\epsilon}_0}{V_0 Q_0}. \tag{9}$$

Substitution yields the equation used for estimation of the amplitude dependent attenuation

$$\Delta(1/Q(\hat{\epsilon}))=\frac{1}{Q(\hat{\epsilon})}-\frac{1}{Q_0}=\frac{1}{Q_0}\left(\frac{V\hat{\epsilon}_0}{V_0\hat{\epsilon}}-1\right), \tag{10}$$

which we use to obtain $\Delta(1/Q(\hat{\epsilon}))$ from measurements.

Numerous observations show that the change in $Q(\hat{\epsilon})$ and resonance frequency $f(\hat{\epsilon})$ scales linearly with strain amplitude[1,5,7] above approximately 10^{-6}, in the ANFD regime. In this strain region, we define α_Q as the parameter relating strain and nonlinear energy loss

$$\frac{1}{Q(\hat{\epsilon})}-\frac{1}{Q_0}=\alpha_Q\hat{\epsilon}. \tag{11}$$

Likewise, we define a parameter describing the frequency shift. In the strain range where ANFD is invoked, we have empirically that

$$\frac{f(\hat{\epsilon})-f_0}{f_0}=\frac{\Delta f(\hat{\epsilon})}{f_0}=\alpha_f\hat{\epsilon}, \tag{12}$$

where α_f relates frequency shift and strain amplitude. The P-M space theory predicts the above two relations as well[14]

as does the theory described in Ref. 25. α_f ranges from 10^2 to 10^4 for the materials where it has been measured.[7] We will apply the earlier equations to calculate the characteristic parameters α_f and α_Q from the experimental data.

Recall that SD is the return to equilibrium after large amplitude dynamic excitation. In our experiments, we first conduct a RUS measurement to probe the equilibrium state, then condition the sample at large amplitude, then probe the sample using RUS over a period of time to observe SD.

Specifically, the equilibrium, low amplitude (linear) resonance frequency f_0 of the sample is measured using a standard, low amplitude, swept-frequency resonance using the DRS device before high-amplitude disturbance. The peak is extracted from a lorenzian fit. The sample is then driven at fixed frequency near a resonance and large strain amplitude corresponding to the maximum amplitudes shown in Table II for 2 min to induce material softening. Immediately upon termination of the drive, the RUS measurement recommences at very low strain amplitude (order microstrain) in order to probe the recovery of the resonant peak frequency and Q as a function of elapsed time.

Here $V=V_0$ due to the fact that we probe with low amplitude frequency-sweeps, so Eq. (10) becomes

$$\frac{1}{Q(t)}-\frac{1}{Q_0}=\frac{1}{Q_0}\left(\frac{\hat{\epsilon}_0}{\hat{\epsilon}(t)}-1\right), \tag{13}$$

where $\hat{\epsilon}_0$ is the final, equilibrium strain. Thus it is only necessary to measure the strain amplitude at each frequency peak in the recovery. These measurements are obtained by measuring the peak of a lorenzian fit for each successive resonance curve taken in time.

The effect of temperature is significant and can influence the SD result if one is not extremely careful.[13] Thus precautions were taken to minimize these effects by employing a temperature stable environment using an insulated box constructed from styrofoam.

Materials tested that do not exhibit ANFD/SD include Pyrex glass, polycarbonate, PVC, 5180 steel, tantalum, aluminum, lucite, martinsitic 5180 steel, and pearlitic 5180 steel. A complete list of materials tested in the reconnaissance experiments is available from the authors.

IV. RESULTS

Figure 3 shows raw resonance curves for ANFD/SD obtained from one of the materials (feldspathic quartzite). Figure 3(a) shows amplitude/frequency response of the strain for progressively increasing levels of excitation. Material softening appears as a change in the resonance frequency with drive voltage. Figure 3(b) shows the same data normalized to the amplitude of the applied voltage. This manner of plotting is valuable in simultaneously isolating resonance frequency change and nonlinear dissipation change with strain level. The fact that the amplitude of the normalized peak decreases with increasing drive level and the resonance peak simultaneously broadens indicates the material nonlinear dissipation is increasing with material softening. Figure 3(c) shows the amplitude/frequency response measured at successively increasing times during the recovery process, the SD, for the same material. Recall the drive is fixed at a very small level (assumed linear elastic) during the SD measurements. The recovery is linear with the logarithm of time, as was seen in Berea sandstone.[3]

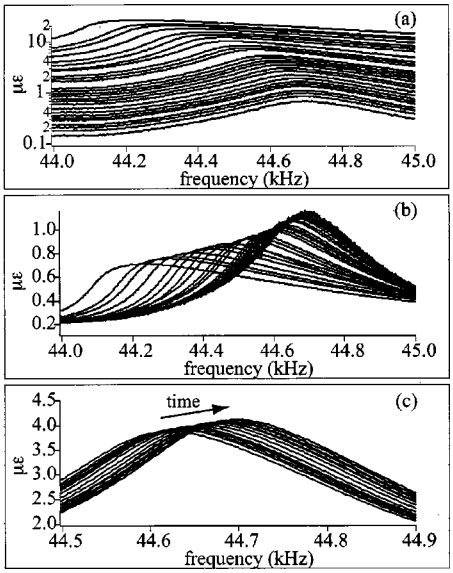

FIG. 3. ANFD and SD observation in the quartzite. (a) shows the resonance curves, (b) shows resonance curves normalized to drive voltage, and (c) shows the SD recovery. Amplitude is in microstrain.

Figures 4(a) and (b) illustrate the change in frequency $(\Delta f/f_0)$ and $Q((1/Q-1/Q_0)$ dependence on strain for all samples obtained from the raw resonance curves. In the low amplitude drive region the dependencies are classically nonlinear [Eq. (3)], and they exhibit nonclassical behavior $[(\Delta f/f_0)$ and $1/Q-1/Q_0$ scale linear with strain] at the higher amplitudes. From the strain region where frequency scales linear with strain amplitude, α_{ANFD} and α_{SD} were extracted.

Table II shows the resonance frequency used, the maximum strain, the material wave speed, and Q_0 for each sample. Table III shows the values of α_f and α_Q extracted from the measurements.

Figures 4(b) and (d) show combined results of frequency and dissipation for SD. In SD, the frequency and $1/Q$ recovers linearly with the log of time.

In order to characterize the relative changes of Q and resonance frequency with strain level in ANFD, we introduce γ_{ANFD}, the ratio of the α parameters: that is, the ratio of the energy loss to the frequency shift ($\gamma_{\mathrm{ANFD}}=\alpha_Q/\alpha_f$). γ_{ANFD} ranges from 0.28 to 1.10 meaning the change in frequency is less than the change in attenuation except in the Pyrex sample. In Berea sandstone, γ_{ANFD} was found to be 0.3.[26]

We note one other observation of interest. We calculated the ratio of the dissipation change to the frequency shift during the SD recovery to see if it had variation between materials. This ratio, termed γ_{SD}, is

$$\gamma_{\mathrm{SD}}=\left(\frac{1}{Q(t)}-\frac{1}{Q_0}\right)\frac{f_0}{\Delta f(t)}. \tag{14}$$

Here $V=V_0$ due to the fact that we probe with low amplitude frequency-sweeps. Substituting using Eq. (13) we get

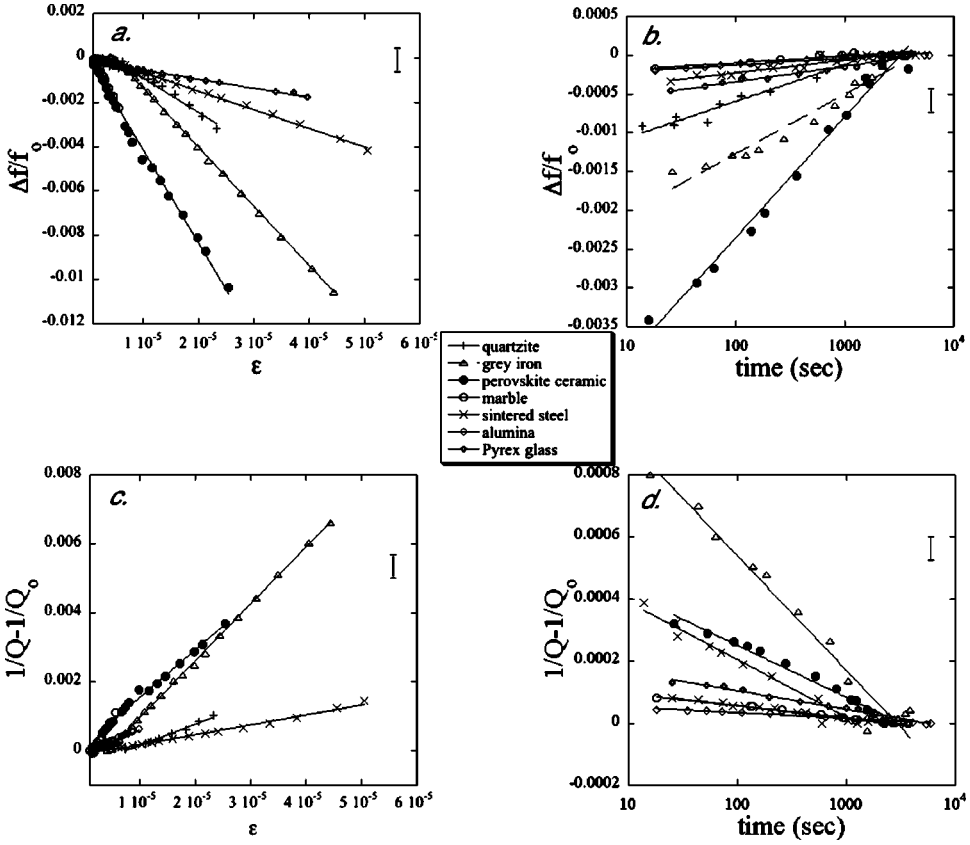

FIG. 4. ANFD and SD in all samples. (a) and (b) show the change in resonance frequency $f-f_0$ normalized to the linear resonance frequency f_0 for ANFD and SD, respectively. (c) and (d) show the behavior in $1/Q$ for ANFD–SD, respectively. The error bars shown are based are extremely conservative: they are obtained from the frequency sampling rate of the experiment, carried through all of the calculations. The lines in the figures are present to guide the eye (they are linear fits in the case of ANFD and logarithmic fits for SD). These data were used to calculate γ_{ANFD} and γ_{SD} in Table III. The high-strain-amplitude data, where $f-f_0$ and $1/Q$ are linear proportional to strain, were used to calculate α in Table III.

$$\gamma_{\mathrm{SD}}=\frac{f}{\Delta f(t)}\left(\frac{1}{Q_0}\frac{\hat{\epsilon}_0}{\hat{\epsilon}(t)}-1\right), \tag{15}$$

where $\hat{\epsilon}_0$ is the final, equilibrium strain. The measured values of this are presented in Table III as well. We find that γ_{SD} are very similar for all seven materials (0.23–0.46). The SD must be due entirely to the relaxation of stored strain assuming the probe wave does not influence the total system strain energy.

V. DISCUSSION

Our primary purpose in this work was to illustrate new observations of ANFD/SD. This is the first systematic study describing ANFD/SD in numerous materials. We find that wherever ANFD are observed, SD are also observed, and vice-versa. We describe results in seven of these materials that represent the huge diversity of the class. We further find that there is a relationship between resonance frequency shift and wave dissipation in ANFD that is similar, but not the same, in each of seven materials. This relation is between 0.28 and 0.66, except for cracked glass which exhibits a ratio of 1.1. The ratios appear to be material dependent. Cracked glass is known to exhibit unusual mechanical behavior in general. We also measure the ratio of dissipation to frequency shift during slow dynamics. This ratio, termed γ_{SD} was between 0.23 and 0.43.

The parameter γ_{ANFD} is predicted by different models. The P-M space[14] model predicts γ_{ANFD} of approximately one, and other hysteretic empirical models such as that described in Ref. 26 leave some flexibility in this value.

In our view, there are currently two credible theoretical approaches that link ANFD/SD. The first is the approach employing a variation of the P-M space model described by Scalerandi and Delsanto.[4] The second is a model described by Vakhnenko *et al.*[16] that treats the elastic nonlinearity of the solid as an ensemble of rupturing bonds.

TABLE II. Sample elastic linear and nonlinear properties for the seven materials studied [Note that Q_0 is the Q of the loaded (source+sample) system]. Wave speed for sintered metal not measured.

Material	f_0 (kHz)	Max strain (10^{-6})	Wave speed (m/s)	Q_0
Pearlite/graphite metal	44.7	44.0	3225	487
Alumina ceramic	9.12	10.0	4940	415
Quartzite	33.6	2.3	3826	167
Pyrex containing cracks	20.0	35.0	4700	662
Marble	86.3	5.6	4030	353
Sintered metal	9.4	5.0		346
Perovskite ceramic	60.0	26.0	1670	140

TABLE III. Values of γ for ANFD and SD in seven materials. α is not shown for the sintered metal part because the strain amplitudes were not directly calculable due to sample geometry, meaning α could not be extracted.

Material	Mean α_Q	Mean α_f	Mean γ_{ANFD}	Mean γ_{SD}
Perlite/graphite metal	487±37	167±25	0.35±0.03	0.25±0.02
Alumina ceramic	95±4	63±14	0.66±0.12	0.26±0.05
Quartzite	145±10	41±7	0.28±0.02	0.36±0.02
Pyrex containing cracks	81±10	84±6	1.10±0.09	0.30±0.02
Marble	370±65	149±45	0.42±0.04	0.43±0.5
Sintered metal			0.31±0.03	0.25±0.03
Perovskite ceramic	240±31	164±11	0.66±0.04	0.23±0.01

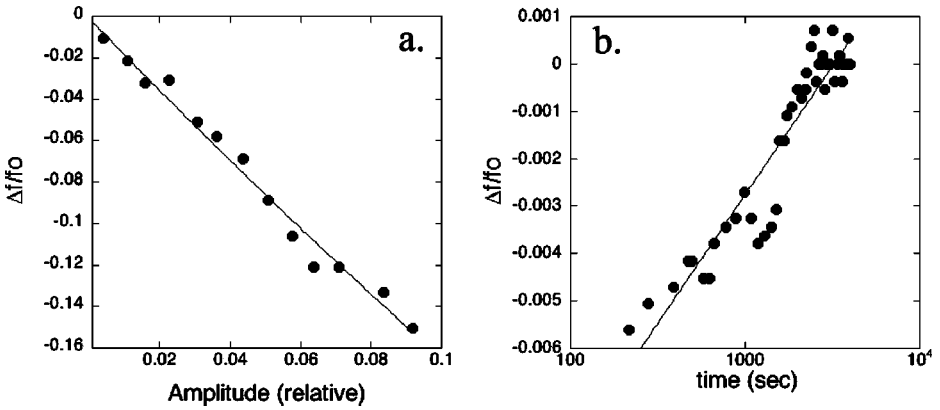

FIG. 5. Model frequency results of ANFD (a) and SD (b).

The reason so few models exist, and in fact that the most widely applied model (P-M space) is phenomenological, is that the physical basis for ANFD/SD is lacking because the origin(s) of these behaviors are unknown. In fact, the physical origins appear to be represented by the spectrum of materials presented in this paper. For instance, dislocations in the metals and glassy dynamics in amorphous materials are likely candidates for the physical origin in these instances; but in cracked glass, sintered metal, or rock, it is not at all clear what could be responsible for the observed behaviors. However, due to the fact that we cannot address the actual physics, we will appeal to the model presented in Refs. 4 and 27 which links ANFD/SD.

The model is based on the local interaction simulation approach[28] applied with a spring model and a version of the Preisach–Mayergoyz (PM) space model of elasticity.[14] In the model the material is described as a sequence of linear elastic elements (the ''hard'' portion—the grain system) and the interstices (the ''soft'' bond system) are described by a large number of hysteretic elastic units that can behave either rigidly or elastically depending on the local pressure. These units correspond to the bond system, localized in the damaged material or distributed in the others. The model includes thermally activated random transitions between different states (rigid or elastic).

This approach is incorporated into PM space where the dynamic wave disturbance is tracked providing the means to predict the dynamic system stress-strain behavior, the ANFD. The SD arise from the fact that the PM space is altered after a wave disturbance, translating to a different bulk material (modulus) state (see Fig. 4 in Scalerandi and Delsanto).[4] The altered material state returns to its initial state with (bulk) log time behavior by thermally activated jumps in state within the hysteretic elastic units from the portion of PM space that has been altered.

From the model, ANFD and SD emerge. Figure 5 shows model results extracted from Scalerandi and Delsanto[4] where the frequency behaviors in ANFD and SD are predicted. They exhibit the same scaling behavior in ANFD as the results shown here, and the log (time) recovery of SD. The general approach appears to capture the properties of ANFD and SD, and could potentially be modified to predict material characteristic behaviors.

We note that, due to the effects of conditioning during ANFD, the rate of conducting a resonance frequency sweep has effects on the shape of the resonance curve.[2] The rate can also affect the resonance peak frequency. We studied the effect by varying the sweep rates and measuring the effect on the calculation of α_f, α_Q, and γ_{ANFD}. We found that the sweep rate can produce variations up to a few percent in these parameters (A quantitative study of sweep-rate dependence is in progress.). We therefore used constant sweep rates in measurements described here. In addition, we conducted the measurements of ANFD at amplitudes much less than those used for the conditioning/SD measurements, where the effects of conditioning are minimized.

VI. CONCLUSIONS

This is the first systematic study showing the relation of ANFD and SD in a large group of solids confirming that, to date, ANFD and SD appear together. We find that, for the seven different materials studied here, γ_{ANFD}, the ratio of internal friction to the resonance frequency shift, has the same order (0.28–0.63). In SD measurements we find that the ratio of internal friction to frequency shift as a function of time during SD, γ_{SD}, has the same order also (0.23–0.43). We do not know the physical basis of ANFD and SD but the fact that they occur together and have the same order of ratio between elastic and anelestic modulus changes point to same physical mechanism for the both effects. Much of our current work is focused on this question.

ACKNOWLEDGMENTS

The work was supported by the US DOE Office of Basic Energy Science. The authors are grateful to invaluable input from S. Habib, M. Scalerandi, P.-P. Delsanto, K. E.-A. Van Den Abeele, D. Pasqualini, K. Heitmann, J. Tencate, R. A. Guyer, and T. Darling.

[1] L. A. Ostrovsky and P. Johnson, ''Dynamic nonlinear elasticity in geomaterials,'' Riv. Nuovo Cimento **24**, 1–46 (2001).
[2] P. A. Johnson, B. Zinszner, and P. N. J. Rasolofosaon, ''Resonance and elastic nonlinear phenomena in rock,'' J. Geophys. Res. **101**, 11553–11564 (1996).
[3] J. TenCate and T. Shankland, ''Slow dynamics in the nonlinear elastic response of Berea sandstone,'' Geophys. Res. Lett. **23**, 3019–3022 (1996).
[4] P.-P. Delsanto and M. Scalerandi, ''Modeling nonclassical nonlinearity, conditioning, and slow dynamics effects in mesoscopic elastic materials,'' Phys. Rev. B **68**, 064107–064116 (2003).
[5] R. A. Guyer and P. Johnson, ''Nonlinear mesoscopic elasticity: Evidence for a new class of materials,'' Phys. Today **52**, 30–36 (1999).

[6] K. E.-A. Van Den Abeele, J. Carmeliet, J. A. Ten Cate, and P. A. Johnson, ''Nonlinear elastic wave spectroscopy (NEWS) techniques to discern material damage, Part II: Single-mode nonlinear resonance acoustic spectroscopy,'' Res. Nondestruct. Eval. **12**, 31–42 (2000).
[7] P. A. Johnson, B. Zinszner, P. Rasolofosaon, K. Van Den Abeele, and F. Cohen-Tenoudji, ''Dynamic measurements of the nonlinear elastic parameter alpha in rock under varying conditions,'' J. Geophys. Res. **109**, 10129–10139 (2004).
[8] J. C. Lacouture, P. Johnson, and F. Cohen-Tenoudji, ''Study of critical behavior in concrete during curing by application of dynamic linear and nonlinear means,'' J. Acoust. Soc. Am. **113**, 1325–1332 (2003).
[9] J. TenCate, D. E. Smith, and R. Guyer, ''Universal slow dynamics in granular solids,'' Phys. Rev. Lett. **85**, 1020–1023 (2000).
[10] P. A. Johnson, A. Sutin, and J. TenCate, ''Development of nonlinear slow dynamical damage diagnostics (S3D) for application to nondestructive evaluation,'' Proceedings of the World Congress on Ultrasonics 2003, pp. 129–132 (http://www.sfa.asso.fr/wcu2003/procs/website/index.html)
[11] V. Zaitsev, B. Castagnede, and V. Gusev, ''Thermoelastic mechanism for logarithmic slow dynamics and memory in elastic wave interactions with individual cracks,'' Phys. Rev. Lett. **90**, 075501–075504 (2003).
[12] L. D. Landau and E. M. Lifschitz, *Theory of Elasticity* (Pergamon, New York, 1986).
[13] J. TenCate, D. Pasqualini, S. Habib, K. Heitmann, P. Johnson, and D. Higdon, ''Nonlinear and nonequilibrium dynamics in geomaterials,'' Phys. Rev. Lett. **93**, 065501–065504 (2004).
[14] K. R. McCall and R. Guyer, ''Equation of state and wave propagation in hysteretic nonlinear elastic materials,'' J. Geophys. Res. **99**, 23887–23897 (1994).
[15] K. E.-A. Van Den Abeele, J. Carmeliet, P. A. Johnson, and B. Zinszner, ''Influence of water saturation on the nonlinear elastic mesoscopic response in Earth materials and the implications to the mechanism of nonlinearity,'' J. Geophys. Res. **107**, 101029–101040 (2002).
[16] O. Vakhnenko, V. Vakhnenko, T. J. Shankland, and J. TenCate, ''Strain-induced kinetics of intergrain defects as the mechanism of slow dynamics in the nonlinear resonant response of humid sandstone bars,'' Phys. Rev. E **70**, 15602–15604 (2004).
[17] U. Hunsche and N. Cristescu, *Time Effects in Rock Mechanics* (Wiley, New York, 1998).
[18] B. I. Pandit and J. C. Savage, ''An experimental test of Lomnitz's theory of internal friction in rocks,'' J. Geophys. Res. **78**, 6097–6099 (1973).
[19] *Creep Behavior of Advanced Materials for the 21st Century*, edited by R. Mishra, A. K. Mukherjee, and K. L. Murty (Minerals, Metals & Materials Society, London, 1999).
[20] K. H. Fischer and J. A. Hertz, *Spin Glasses* (Cambridge University Press, Cambridge, 1991), p. 8.
[21] N. Toksoz and D. Johnston, *Seismic Wave Attenuation* (Geophysics Reprints Series No. 2, Tulsa, 1982).
[22] D. O. Thompson and F. M. Glass, ''Elastic constant-internal friction spectrometer,'' Rev. Sci. Instrum. **29**, 1034–1040 (1958).
[23] A. L. Audenino and P. M. Calderale, ''Measurement of non-linear internal damping in metals: Processing of decay signals in a uniaxial stress field,'' J. Sound Vib. **198**, 395–409 (1996).
[24] R. De Batist, *Internal Friction of Structural Defects in Crystalline Solids* (North Holland, London, 1972).
[25] V. E. Nazarov, A. V. Radostin, L. A. Ostrovsky, and I. A. Soustova, ''Wave processes in media with hysteretic nonlinearity: Part 2,'' Acoust. Phys. **49**, 444–448 (2003).
[26] R. Guyer, J. TenCate, and P. A. Johnson, ''Hysteresis and the dynamic elasticity of consolidated granular materials,'' Phys. Rev. Lett. **82**, 3280–3283 (1999).
[27] M. Nobili and M. Scalerandi, ''Temperature effects on the elastic properties of hysteretic elastic media: Modeling and simulation,'' Phys. Rev. B **69**, 104105–104116 (2004).
[28] R. S. Schechter, H. H. Chaskelis, R. B. Mignogna, and P. P. Delsanto, ''Real-time parallel computation and visualization of ultrasonic pulses in solids,'' Science **265**, 1188–1192 (1994).